CLEO CONF 99-16

Measurement of Charge Asymmetries in Charmless Hadronic B Decay

CLEO Collaboration

(August 6th, 1999)

Abstract

We search for CP violating asymmetries in the charmless hadronic B meson decays to $K^{\pm}\pi^{\mp}$, $K^{\pm}\pi^{0}$, $K^{0}_{S}\pi^{\pm}$, $K^{\pm}\eta'$, and $\omega\pi^{\pm}$. With the full CLEO II and CLEO II.V datasets statistical precision on $\mathcal{A}_{\rm CP}$ is in the range of ± 0.12 to ± 0.25 depending on the mode. All quoted results are preliminary.

T. E. Coan,[1] V. Fadeyev,[1] I. Korolkov,[1] Y. Maravin,[1] I. Narsky,[1] R. Stroynowski,[1]
J. Ye,[1] T. Wlodek,[1] M. Artuso,[2] R. Ayad,[2] E. Dambasuren,[2] S. Kopp,[2]
G. Majumder,[2] G. C. Moneti,[2] R. Mountain,[2] S. Schuh,[2] T. Skwarnicki,[2]
S. Stone,[2] A. Titov,[2] G. Viehhauser,[2] J.C. Wang,[2] A. Wolf,[2] J. Wu,[2]
S. E. Csorna,[3] K. W. McLean,[3] S. Marka,[3] Z. Xu,[3] R. Godang,[4] K. Kinoshita,[4,1]
I. C. Lai,[4] P. Pomianowski,[4] S. Schrenk,[4] G. Bonvicini,[5] D. Cinabro,[5] R. Greene,[5]
L. P. Perera,[5] G. J. Zhou,[5] S. Chan,[6] G. Eigen,[6] E. Lipeles,[6] M. Schmidtler,[6]
A. Shapiro,[6] W. M. Sun,[6] J. Urheim,[6] A. J. Weinstein,[6] F. Würthwein,[6]
D. E. Jaffe,[7] G. Masek,[7] H. P. Paar,[7] E. M. Potter,[7] S. Prell,[7] V. Sharma,[7]
D. M. Asner,[8] A. Eppich,[8] J. Gronberg,[8] T. S. Hill,[8] D. J. Lange,[8]
R. J. Morrison,[8] T. K. Nelson,[8] J. D. Richman,[8] R. A. Briere,[9] B. H. Behrens,[10]
W. T. Ford,[10] A. Gritsan,[10] H. Krieg,[10] J. Roy,[10] J. G. Smith,[10]
J. P. Alexander,[11] R. Baker,[11] C. Bebek,[11] B. E. Berger,[11] K. Berkelman,[11]
F. Blanc,[11] V. Boisvert,[11] D. G. Cassel,[11] M. Dickson,[11] P. S. Drell,[11]
K. M. Ecklund,[11] R. Ehrlich,[11] A. D. Foland,[11] P. Gaidarev,[11] L. Gibbons,[11]
B. Gittelman,[11] S. W. Gray,[11] D. L. Hartill,[11] B. K. Heltsley,[11] P. I. Hopman,[11]
C. D. Jones,[11] D. L. Kreinick,[11] T. Lee,[11] Y. Liu,[11] T. O. Meyer,[11] N. B. Mistry,[11]
C. R. Ng,[11] E. Nordberg,[11] J. R. Patterson,[11] D. Peterson,[11] D. Riley,[11]
J. G. Thayer,[11] P. G. Thies,[11] B. Valant-Spaight,[11] A. Warburton,[11] P. Avery,[12]
M. Lohner,[12] C. Prescott,[12] A. I. Rubiera,[12] J. Yelton,[12] J. Zheng,[12]
G. Brandenburg,[13] A. Ershov,[13] Y. S. Gao,[13] D. Y.-J. Kim,[13] R. Wilson,[13]
T. E. Browder,[14] Y. Li,[14] J. L. Rodriguez,[14] H. Yamamoto,[14] T. Bergfeld,[15]
B. I. Eisenstein,[15] J. Ernst,[15] G. E. Gladding,[15] G. D. Gollin,[15] R. M. Hans,[15]
E. Johnson,[15] I. Karliner,[15] M. A. Marsh,[15] M. Palmer,[15] C. Plager,[15]
C. Sedlack,[15] M. Selen,[15] J. J. Thaler,[15] J. Williams,[15] K. W. Edwards,[16]
R. Janicek,[17] P. M. Patel,[17] A. J. Sadoff,[18] R. Ammar,[19] P. Baringer,[19] A. Bean,[19]
D. Besson,[19] R. Davis,[19] S. Kotov,[19] I. Kravchenko,[19] N. Kwak,[19] X. Zhao,[19]
S. Anderson,[20] V. V. Frolov,[20] Y. Kubota,[20] S. J. Lee,[20] R. Mahapatra,[20]
J. J. O'Neill,[20] R. Poling,[20] T. Riehle,[20] A. Smith,[20] S. Ahmed,[21] M. S. Alam,[21]
S. B. Athar,[21] L. Jian,[21] L. Ling,[21] A. H. Mahmood,[21,2] M. Saleem,[21] S. Timm,[21]
F. Wappler,[21] A. Anastassov,[22] J. E. Duboscq,[22] K. K. Gan,[22] C. Gwon,[22]
T. Hart,[22] K. Honscheid,[22] H. Kagan,[22] R. Kass,[22] J. Lorenc,[22] H. Schwarthoff,[22]
E. von Toerne,[22] M. M. Zoeller,[22] S. J. Richichi,[23] H. Severini,[23] P. Skubic,[23]
A. Undrus,[23] M. Bishai,[24] S. Chen,[24] J. Fast,[24] J. W. Hinson,[24] J. Lee,[24]
N. Menon,[24] D. H. Miller,[24] E. I. Shibata,[24] I. P. J. Shipsey,[24] Y. Kwon,[25,3]
A.L. Lyon,[25] E. H. Thorndike,[25] C. P. Jessop,[26] K. Lingel,[26] H. Marsiske,[26]
M. L. Perl,[26] V. Savinov,[26] D. Ugolini,[26] and X. Zhou[26]

[1]Southern Methodist University, Dallas, Texas 75275

[1]Permanent address: University of Cincinnati, Cincinnati OH 45221
[2]Permanent address: University of Texas - Pan American, Edinburg TX 78539.
[3]Permanent address: Yonsei University, Seoul 120-749, Korea.

[2]Syracuse University, Syracuse, New York 13244
[3]Vanderbilt University, Nashville, Tennessee 37235
[4]Virginia Polytechnic Institute and State University, Blacksburg, Virginia 24061
[5]Wayne State University, Detroit, Michigan 48202
[6]California Institute of Technology, Pasadena, California 91125
[7]University of California, San Diego, La Jolla, California 92093
[8]University of California, Santa Barbara, California 93106
[9]Carnegie Mellon University, Pittsburgh, Pennsylvania 15213
[10]University of Colorado, Boulder, Colorado 80309-0390
[11]Cornell University, Ithaca, New York 14853
[12]University of Florida, Gainesville, Florida 32611
[13]Harvard University, Cambridge, Massachusetts 02138
[14]University of Hawaii at Manoa, Honolulu, Hawaii 96822
[15]University of Illinois, Urbana-Champaign, Illinois 61801
[16]Carleton University, Ottawa, Ontario, Canada K1S 5B6
and the Institute of Particle Physics, Canada
[17]McGill University, Montréal, Québec, Canada H3A 2T8
and the Institute of Particle Physics, Canada
[18]Ithaca College, Ithaca, New York 14850
[19]University of Kansas, Lawrence, Kansas 66045
[20]University of Minnesota, Minneapolis, Minnesota 55455
[21]State University of New York at Albany, Albany, New York 12222
[22]Ohio State University, Columbus, Ohio 43210
[23]University of Oklahoma, Norman, Oklahoma 73019
[24]Purdue University, West Lafayette, Indiana 47907
[25]University of Rochester, Rochester, New York 14627
[26]Stanford Linear Accelerator Center, Stanford University, Stanford, California 94309

1 Introduction

CP violating phenomena arise in the Standard Model because of the single complex parameter in the quark mixing matrix.[1] Such phenomena are expected to occur widely in B meson decays and are the incentive for most of the current B-physics initiatives in the world. As of yet there is little direct experimental evidence. CDF's recent determination[2] of $\sin 2\beta$ at the 2σ level, which followed upon earlier less sensitive searches by both CDF[3] and OPAL[4], is consistent with expectations for mixing-induced Standard Model CP violation and to date the only evidence of CP effects in B mesons.

Direct CP violation however is also anticipated to play a prominent role in the CP phenomena of B decay. To date the only published search for direct CP violation in B decay is the recent CLEO limit[5] on $\mathcal{A}_{\rm CP}$ in $b \to s\gamma$. CP asymmetries may show up in any mode where there are two or more participating diagrams which differ in weak and strong phases. $B \to K\pi$ modes, for instance, involve $b \to u$ tree diagrams carrying the weak phase $\mathrm{Arg}(V_{ub}^* V_{us}) \equiv \gamma$ and $b \to s$ penguin diagrams carrying the weak phase $\mathrm{Arg}(V_{tb}^* V_{ts}) = \pi$. Though the branching ratios are small, such cases are experimentally straightforward to search for. Rate differences between $B \to K^+\pi^-$ and $\bar{B} \to K^-\pi^+$ decays would be unambiguous signals of direct CP violation if seen.

We report here five searches for direct CP violation in charmless hadronic B decay modes, based on the full CLEO II and CLEO II.V datasets which together comprise 9.66 million $B\bar{B}$ events. The modes searched for are the three $K\pi$ modes, $K^\pm\pi^\mp$, $K^\pm\pi^0$, $K_S^0\pi^\pm$, the mode $K^\pm\eta'$, and the vector-pseudoscalar mode $\omega\pi^\pm$. In all but the first case the flavor of the parent b or $\bar{b}$ quark is tagged simply by the sign of the high momentum charged hadron; for $K^\pm\pi^\mp$ one must further identify K and π.

In what follows we will refer when needed to the generic final state from b and $\bar{b}$ as f and $\bar{f}$ respectively. The corresponding event yields of signal and background we will label as $\mathcal{S}$, $\overline{\mathcal{S}}$, $\mathcal{B}$, and $\overline{\mathcal{B}}$. We define the sign of $\mathcal{A}_{\rm CP}$ with the following convention:

$$\mathcal{A}_{\rm CP} \equiv \frac{Br(b \to f) - Br(\bar{b} \to \bar{f})}{Br(\bar{b} \to \bar{f}) + Br(b \to f)} \;=\; \frac{\mathcal{S} - \overline{\mathcal{S}}}{\mathcal{S} + \overline{\mathcal{S}}} \tag{1}$$

The statistical precision one can achieve in a measurement of $\mathcal{A}_{\rm CP}$ depends on the signal yield $S \equiv \mathcal{S} + \overline{\mathcal{S}}$, the CP-symmetric background $B = \mathcal{B} + \overline{\mathcal{B}}$, any correlation χ that might exist between the measurements of f and $\bar{f}$, and of course on $\mathcal{A}_{\rm CP}$ itself:

$$\sigma^2_{\mathcal{A}_{\rm CP}} = \frac{1 - {\mathcal{A}_{\rm CP}}^2}{S}\left(1 + \frac{B}{S}\left(\frac{1 + {\mathcal{A}_{\rm CP}}^2}{1 - {\mathcal{A}_{\rm CP}}^2}\right) - 2\chi\sqrt{\frac{1 - {\mathcal{A}_{\rm CP}}^2}{4} + \frac{B^2}{S^2} + \frac{B}{S}}\right) \tag{2}$$

In most cases there is no chance of confusing f and $\bar{f}$ so $\chi = 0$. However for $f = K^-\pi^+$ and $\bar{f} = K^+\pi^-$, a small degree of crossover is possible due to imperfect particle identification; we find $\chi = -0.11$ for this case. For $\chi \sim 0$, $B/S \sim 1$, and $\mathcal{A}_{\rm CP} \sim 0$ one has an easy rule of thumb, $\sigma \approx \sqrt{2/S}$. For $S \sim 100$ this means one expects statistical precision in the neighborhood of ± 0.15. As will be discussed later, systematic errors are small, and consequently the precision in $\mathcal{A}_{\rm CP}$ measurements can be expected to be dominated by statistical errors for a long time to come. As can be seen in Eq. 2 the

statistical error is in turn dominated by the leading $1/\sqrt{S}$ coefficient which reminds us that the only path to better $\mathcal{A}_{\rm CP}$ measurements will be more data. Improvements to analysis technique that reduce B/S or χ have less impact.

2 Theoretical Expectations

The existence of a CP violating rate asymmetry depends on having both two different CP nonconserving weak phases and two different CP conserving strong phases. The former may arise from either the Standard Model CKM matrix or from new physics, while the latter may arise from the absorptive part of a penguin diagram or from final state interaction effects. The difficulty of calculating strong interaction phases, particularly when long distance non-perturbative effects are involved, largely precludes reliable predictions. Under well-defined model assumptions, however, numerical estimates may be made and the dependence on both model parameters and CKM parameters can be probed. A recent and comprehensive review of CP asymmetries under the assumption of generalized factorization has been published by Ali *et al* [6]. We quote in Table 1 their predictions for the modes examined in this paper.

Mode	$\mathcal{A}_{\rm CP}$
$B \to K^{\pm}\pi^{\mp}$	$0.037 \to 0.106$
$B \to K^{\pm}\pi^{0}$	$0.026 \to 0.092$
$B \to K^{0}\pi^{\pm}$	0.015
$B \to K^{\pm}\eta'$	$0.020 \to 0.061$
$B \to \omega\pi^{\pm}$	$-0.120 \to 0.024$

Table 1: CP asymmetry predictions. The range of $\mathcal{A}_{\rm CP}$ values reflects a range of model parameters. CKM parameters ρ and η are set to $\rho = 0.12$, $\eta = 0.34$. Taken from Ali *et al*, Ref. 6, with signs changed to match the convention of Eq. 1.

If final state interactions are not neglected, however, strong phases as large as 90° are not ruled out and $|\mathcal{A}_{\rm CP}|$ could reach 0.44 in favorable cases.[7] In this nonperturbative regime numerical predictivity is limited, but a variety of relationships among asymmetries or $f, \bar{f}$ rate differences can be found in the literature.[8]

3 Data Set, Detector, Event Selection

The data set used in this analysis was collected with the CLEO II and CLEO II.V detectors at the Cornell Electron Storage Ring (CESR). It consists of 9.1 fb^{-1} taken at the Υ(4S) (on-resonance) and 4.5 fb^{-1} taken below $B\bar{B}$ threshold. The below-threshold sample is used for continuum background studies. The on-resonance sample contains 9.66 million $B\bar{B}$ pairs. This is a factor 2.9 increase in the number of $B\bar{B}$ pairs over the published measurements of the modes considered here [15],[16],[17]. In addition,

the CLEO II.V data set, which has significantly improved particle identification and momentum resolution as compared with CLEO II, now dominates the data set.

CLEO II and CLEO II.V are general purpose solenoidal magnet detectors, described in detail elsewhere [10]. In CLEO II, the momenta of charged particles are measured in a tracking system consisting of a 6-layer straw tube chamber, a 10-layer precision drift chamber, and a 51-layer main drift chamber, all operating inside a 1.5 T superconducting solenoid. The main drift chamber also provides a measurement of the specific ionization loss, dE/dx, used for particle identification. For CLEO II.V the 6-layer straw tube chamber was replaced by a 3-layer, double-sided silicon vertex detector, and the gas in the main drift chamber was changed from an argon-ethane to a helium-propane mixture. Photons are detected using 7800-crystal CsI(Tl) electromagnetic calorimeter. Muons are identified using proportional counters placed at various depths in the steel return yoke of the magnet.

Charged tracks are required to pass track quality cuts based on the average hit residual and the impact parameters in both the $r-\phi$ and $r-z$ planes. Candidate K^0_S are selected from pairs of tracks forming well-measured displaced vertices. Furthermore, we require the K^0_S momentum vector to point back to the beam spot and the $\pi^+\pi^-$ invariant mass to be within 10 MeV, two standard deviations (σ), of the K^0_S mass. Isolated showers with energies greater than 40 MeV in the central region of the CsI calorimeter and greater than 50 MeV elsewhere, are defined to be photons. Pairs of photons with an invariant mass within 2.5σ of the nominal π^0 (η) mass are kinematically fitted with the mass constrained to the nominal π^0 (η) mass. To reduce combinatoric backgrounds we require the lateral shapes of the showers to be consistent with those from photons. To suppress further low energy showers from charged particle interactions in the calorimeter we apply a shower-energy-dependent isolation cut.

Charged particles are identified as kaons or pions using dE/dx. Electrons are rejected based on dE/dx and the ratio of the track momentum to the associated shower energy in the CsI calorimeter. We reject muons by requiring that the tracks do not penetrate the steel absorber to a depth greater than seven nuclear interaction lengths. We have studied the dE/dx separation between kaons and pions for momenta $p \sim 2.6$ GeV/c in data using $D^0 \to K^-\pi^+(\pi^0)$ decays; we find a separation of (1.7 ± 0.1) σ for CLEO II and (2.0 ± 0.1) σ for CLEO II.V.

Resonances are reconstructed through the decay channels: $\eta' \to \eta\pi^+\pi^-$ with $\eta \to \gamma\gamma$; $\eta' \to \rho\gamma$ with $\rho \to \pi^+\pi^-$; and $\omega \to \pi^+\pi^-\pi^0$.

4 Analysis

The $\mathcal{A}_{\rm CP}$ analyses presented are intimately related to the corresponding branching ratio determinations presented in separate contributions to this conference.[9] We summarize here the main points of the analysis.

We select hadronic events and impose efficient quality cuts on tracks, photons, π^0 candidates, and K^0_S candidates. We calculate a beam-constrained B mass $M = \sqrt{E^2_{\rm b} - p^2_B}$, where p_B is the B candidate momentum and $E_{\rm b}$ is the beam energy. The resolution in M ranges from 2.5 to 3.0 MeV/c^2, where the larger resolution corresponds to the

$B^\pm \to h^\pm\pi^0$ decay. We define $\Delta E = E_1 + E_2 - E_{\rm b}$, where E_1 and E_2 are the energies of the daughters of the B meson candidate. The resolution on ΔE is mode-dependent. For final states without photons the ΔE resolution for CLEO II.V(II) is 20(26) MeV. Most other modes are only slightly worse but for the $B^\pm \to h^\pm\pi^0$ analysis, the ΔE resolution is worse by about a factor of two and becomes asymmetric because of energy loss out of the back of the CsI crystals. The energy constraint also helps to distinguish between modes of the same topology. For example, ΔE for $B \to K^+\pi^-$, calculated assuming $B \to \pi^+\pi^-$, has a distribution that is centered at -42 MeV, giving a separation of $2.1(1.6)\sigma$ between $B \to K^+\pi^-$ and $B \to \pi^+\pi^-$ for CLEO II.V(II). We accept events with M within $5.2 - 5.3$ GeV/c^2 and $|\Delta E| < 200$ MeV. The ΔE requirement is loosened to 300 MeV for the $B^\pm \to h^\pm\pi^0$ analysis. This fiducial region includes the signal region, and a sideband for background determination. Similar regions are included around each of the resonance masses (η', η, and ω) in the likelihood fit. For the $\eta' \to \rho\gamma$ case, the ρ mass is not included in the fit; we require 0.5 GeV $< m_{\pi\pi} <$ 0.9 GeV.

We have studied backgrounds from $b \to c$ decays and other $b \to u$ and $b \to s$ decays and find that all are negligible for the analyses presented here. The main background arises from $e^+e^- \to q\bar{q}$ (where $q = u, d, s, c$). Such events typically exhibit a two-jet structure and can produce high momentum back-to-back tracks in the fiducial region. To reduce contamination from these events, we calculate the angle θ_{sph} between the sphericity axis[11] of the candidate tracks and showers and the sphericity axis of the rest of the event. The distribution of $\cos\theta_{\rm sph}$ is strongly peaked at ± 1 for $q\bar{q}$ events and is nearly flat for $B\bar{B}$ events. We require $|\cos\theta_{\rm sph}| < 0.8$ which eliminates 83% of the background. For η' and ω modes the cut is made at 0.9.

Additional discrimination between signal and $q\bar{q}$ background is provided by a Fisher discriminant technique as described in detail in Ref. [13]. The Fisher discriminant is a linear combination $\mathcal{F} \equiv \sum_{i=1}^{N} \alpha_i y_i$ where the coefficients α_i are chosen to maximize the separation between the signal and background Monte-Carlo samples. The 11 inputs, y_i, are $|\cos\theta_{cand}|$ (the cosine of the angle between the candidate sphericity axis and beam axis), the ratio of Fox-Wolfram moments H_2/H_0 [14], and nine variables that measure the scalar sum of the momenta of tracks and showers from the rest of the event in nine angular bins, each of 10°, centered about the candidate's sphericity axis. For the η' and ω modes, $|\cos\theta_B|$ (the angle between the B meson momentum and beam axis), is used instead of H_2/H_0.

Using a detailed GEANT-based Monte-Carlo simulation [12] we determine overall detection efficiencies of $15 - 46\%$, as listed in Table 2. Efficiencies contain secondary branching fractions for $K^0 \to K^0_S \to \pi^+\pi^-$ and $\pi^0 \to \gamma\gamma$ as well as η' and ω decay modes where applicable. We estimate a systematic error on the efficiency using independent data samples.

In Table 2 we summarize, for each mode, cuts, efficiencies, and the total number of events which pass the cuts and enter the likelihood fit described in the next paragraph.

To extract signal and background yields we perform unbinned maximum-likelihood (ML) fits using ΔE, M, $\mathcal{F}$, $|\cos\theta_B|$ (if not used in $\mathcal{F}$), and dE/dx (where applicable), daughter resonance mass (where applicable), and helicity angle in the daughter decay (where applicable). The free parameters to be fitted are the asymmetry $((f - \bar{f})/(f +$

	$K^{\pm}\pi^0$	$K^0\pi^{\pm}$	$\omega\pi^{\pm}$	$\eta' K^{\pm}$		$K^{\pm}\pi^{\mp}$
				$\eta\pi^+\pi^-$	$\rho\gamma$	
M_B	5.2-5.3	5.2-5.3	5.2-5.3	5.2-5.3	5.2 5.3	5.2-5.3
$\lvert\Delta E\rvert$	< 0.3	< 0.2	< 0.2	< 0.2	< 0.2	< 0.2
$\lvert\cos\theta_{\rm sph}\rvert$	< 0.8	< 0.8	< 0.9	< 0.9	< 0.9	< 0.8
Efficiency	0.40	0.15	0.26	0.27	0.29	0.46
Events in Fit	6991	1558	21337	395	10284	5407

Table 2: Summary of cuts and number of events used in each mode.

$\bar{f}$)) and the sum $(f + \bar{f})$ in both signal and background. In most cases there is more than one possible signal component and its corresponding background component, as for instance we fit simultaneously for $K^+\pi^0$ and $\pi^+\pi^0$ to ensure proper handling of the $K\pi$ identification information. The probability distribution functions (PDFs) describing the distribution of events in each variable are parametrized by simple forms (gaussians, polynomials, etc.) whose parameter values are determined in separate studies. For signal PDF shapes the parameter determinations are made by fitting signal Monte Carlo events. Backgrounds in these analyses are dominated by continuum $ee \to q\bar{q}$ events, and we determine parameters of the background PDFs by fitting data taken below the $\Upsilon(4S)$ resonance or data taken on resonance but lying in the sidebands of the signal region. The uncertainties associated with such fits are used later to assess the final systematic error.

5 Results

($K\pi^0$) In the mode $B^{\pm} \to K^{\pm}\pi^0$ we find a total of $45.6^{+11.2}_{-10.2}$ events with an asymmetry of $\mathcal{A}_{\rm CP}(K\pi^0) = -0.27 \pm 0.23$. This corresponds to 28.9 ± 7.5 $K^+\pi^0$ and 16.8 ± 7.5 $K^-\pi^0$ events. (Here and elsewhere we will quote the yields $\mathcal{S}$ and $\overline{\mathcal{S}}$ for the convenience of the reader. These are derivative quantities as the fit directly extracts $\mathcal{A}_{\rm CP}$ and $\mathcal{S} + \overline{\mathcal{S}}$.) We note that $\pi\pi^0$ which is analyzed simultaneously but does not have a sufficiently significant yield to measure a branching fraction shows an asymmetry of $\mathcal{A}_{\rm CP}(\pi\pi^0) = -0.03 \pm 0.40$. Fig. 1 shows the likelihood function dependence on $\mathcal{A}_{\rm CP}(K\pi^0)$. As a cross check we measure the asymmetry of the background events, finding 0.023 ± 0.026 for $K\pi^0$ background and 0.000 ± 0.017 for $\pi\pi^0$ background. These values are consistent with the expected null result for continuum background.

($K_s\pi$) In the mode $B^{\pm} \to K_s\pi^{\pm}$ we find a total of $25.2^{+6.4}_{-5.6}$ events with an asymmetry of $\mathcal{A}_{\rm CP}(K_s\pi) = 0.17 \pm 0.24$. This corresponds to 10.2 ± 4.0 $K_s\pi^+$ and 14.5 ± 4.4 $K_s\pi^-$ events. The background events show an asymmetry of -0.02 ± 0.04, consistent with zero as expected.

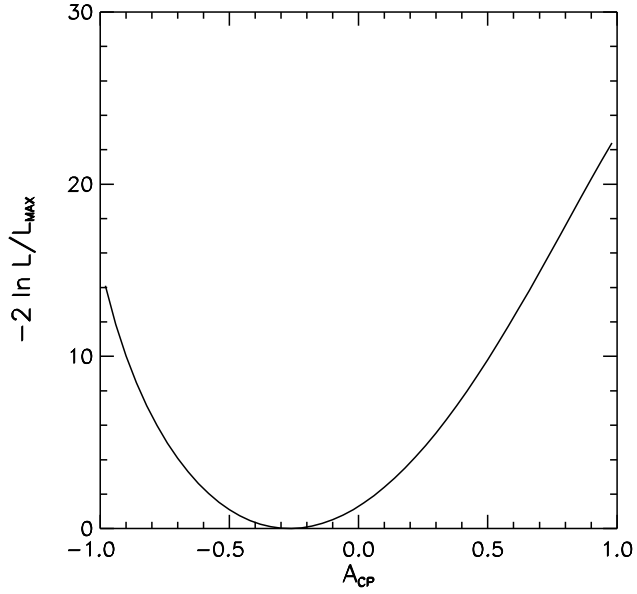

Figure 1: $B \to K^{\pm}\pi^0$ mode: $-2\ln(\mathcal{L}/\mathcal{L}_{max})$ as a function of $\mathcal{A}_{\rm CP}$.

$(K\pi)$ In the mode $B \to K^{\pm}\pi^{\mp}$ we find a total of $80.2^{+11.8}_{-11.0}$ events with an asymmetry of $\mathcal{A}_{\rm CP}(K\pi) = -0.04 \pm 0.16$. This corresponds to $41.6^{+8.9}_{-8.0}$ $K^+\pi^-$ and $38.6^{+9.0}_{-8.1}$ $K^-\pi^+$ events. The dependence of the likelihood function on $\mathcal{A}_{\rm CP}$ is shown in Fig. 2. The background events show an asymmetry of -0.02 ± 0.04, consistent with zero as expected.

$(\omega\pi)$ In the mode $B^{\pm} \to \omega\pi^{\pm}$ we find a total of $28.5^{+8.2}_{-7.3}$ events with $\mathcal{A}_{\rm CP}(\omega\pi) = -0.34^{+0.24}_{-0.26}$. This corresponds to $19.1^{+6.8}_{-5.9}$ $\omega\pi^+$ events and $9.4^{+4.9}_{-4.0}$ $\omega\pi^-$ events. Figure 3 shows the likelihood as a function of $\mathcal{A}_{\rm CP}$. The fit also allows for a possible charge asymmetry in the continuum background, and finds values consistent with zero: -0.013 ± 0.015 for $\omega K^{\pm}$ background, and -0.001 ± 0.010 for $\omega\pi^{\pm}$ background.

$(\eta' K)$ We find $\mathcal{A}_{\rm CP}(\eta' K) = 0.03 \pm 0.12$. Separating the $\eta' K$ signal sample by submodes $\eta' \to \eta\pi^+\pi^-$ and $\eta' \to \rho\gamma$ we find $\mathcal{A}_{\rm CP} = 0.06 \pm 0.17$ and $\mathcal{A}_{\rm CP} = -0.01 \pm 0.17$, respectively. Fig. 4 shows the dependence of the fitted likelihood function on $\mathcal{A}_{\rm CP}$ for the separate and combined submodes. Background $\eta' K$ events are found to have an asymmetry of -0.01 ± 0.07 in the $\eta\pi^+\pi^-$ mode, and -0.009 ± 0.015 in the $\rho\gamma$ mode, both consistent with zero as expected.

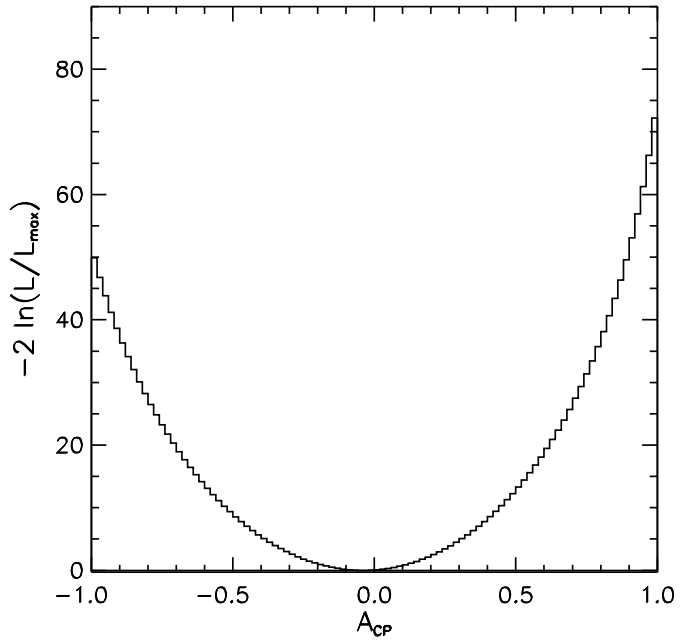

Figure 2: $K^{\pm}\pi^{\mp}$ mode: $-2\ln(\mathcal{L}/\mathcal{L}_{max})$ plotted versus $\mathcal{A}_{\rm CP}$.

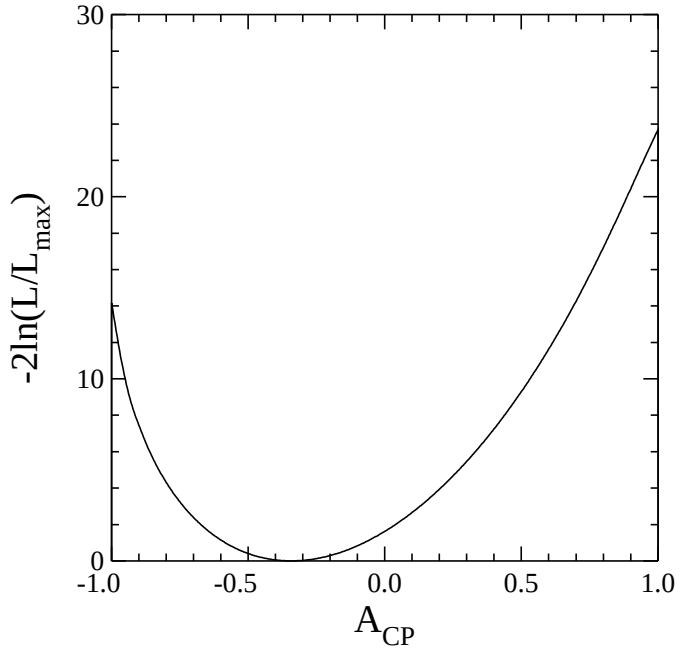

Figure 3: $B^{\pm} \to \omega\pi^{\pm}$ mode: $-2\ln(\mathcal{L}/\mathcal{L}_{max})$ as a function of $\mathcal{A}_{\rm CP}$.

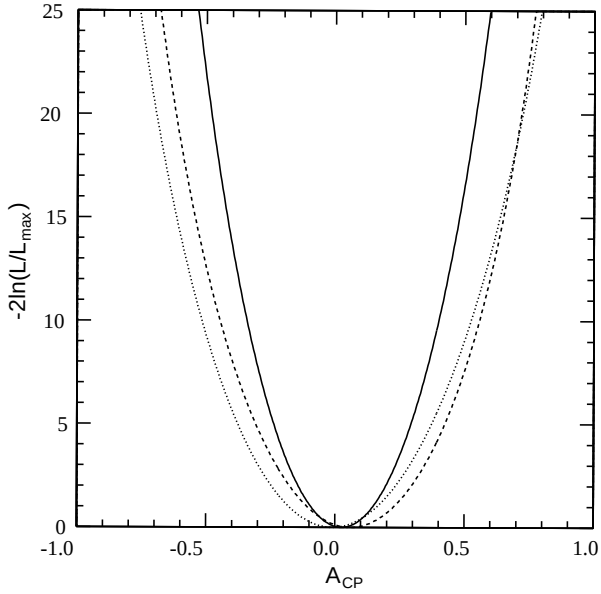

Figure 4: $\eta' K^{\pm}$ mode: $-2\ln(\mathcal{L}/\mathcal{L}_{max})$ plotted versus $\mathcal{A}_{\rm CP}$. The dashed curve shows the fit result for the $\eta' \to \eta\pi\pi$ decay, the dotted curve for $\eta' \to \rho\gamma$ and the solid curve is the combined result.

6 Systematic Errors

The charge asymmetries measured in this analysis hinge primarily on the properties of high momentum tracks. The charged meson that tags the parent $b/\bar{b}$ flavor has momentum in all cases between 2.3 and 2.8 GeV/c. In independent studies using very large samples of high momentum tracks we have searched for and set stringent limits on the extent of possible charge-correlated bias in the CLEO detector and analysis chain for tracks in the $2-3$GeV range. Based on a sample of 8 million tracks, we find $\mathcal{A}_{\rm CP}$ bias introduced by differences in reconstruction efficiencies for positive and negative high momentum tracks passing the same track quality requirements as are imposed in this analysis is less than ± 0.002. For $K^{\pm}\pi^{\mp}$ combinations where differential charge-correlated efficiencies must also be considered in correlation with K/π flavor, we use 37,000 $D^0 \to K\pi(\pi^0)$ decays and set a corresponding limit on $\mathcal{A}_{\rm CP}$ bias at ± 0.005. These D^0 decays, together with an additional 24,000 $D^{\pm}_{(s)}$ decays, are also used to set a tight upper limit of 0.4 MeV/c on any charge-correlated or charge-strangeness-correlated bias in momentum measurement. The resulting limit on $\mathcal{A}_{\rm CP}$ bias from this source is ± 0.002. We conclude that there is no significant $\mathcal{A}_{\rm CP}$ bias introduced by track reconstruction or selection. We note that for each mode we crosscheck the asymmetry of the background events

(normally a fairly large sample) and find results consistent with zero as anticipated.

Particle identification information for $K^{\pm}$ and $\pi^{\pm}$ is shown in Fig. 5. No significant differences are seen between different charge species. Quantification of the effect on $\mathcal{A}_{\rm CP}$ is covered by PDF variation studies discussed immediately below.

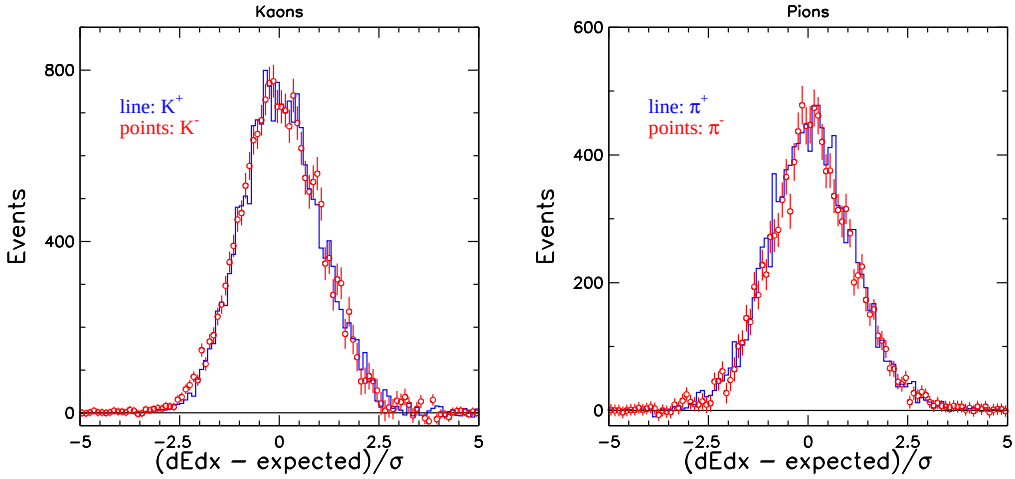

Figure 5: Normal central dE/dx distributions for $K^{\pm}$ and $\pi^{\pm}$.

All PDF shapes which are used in the maximum likelihood fits are varied within limits prescribed by the fits which determine the shape parameters to assess the systematic error associated with uncertainty in the parameters. The resulting changes in $\mathcal{A}_{\rm CP}$ are summed in quadrature to estimate the systematic error due to possible misparametrization of the PDF shapes. This contribution to the systematic error ranges from ± 0.02 to ± 0.04 depending on mode.

We choose to assign a conservative systematic error ± 0.05 for all modes.

7 Summary

Table 3 and Fig. 6 summarize all results.

We have presented in this paper the first measurements of charge asymmetries in hadronic B decay. We see no evidence for CP violation in the five modes analyzed here and set 90% CL intervals (systematics included) that reduce the possible range of $\mathcal{A}_{\rm CP}$ by as much as a factor of four. While the sensitivity is not yet sufficient to address the rather small $\mathcal{A}_{\rm CP}$ values predicted by factorization models, extremely large $\mathcal{A}_{\rm CP}$ values which could arise if large phases were available from final state interactions are firmly ruled out. For the case of $K\pi$ and $\eta' K$ we can exclude at 90% confidence values of $|\mathcal{A}_{\rm CP}|$ greater than 0.35 and 0.28 respectively.

Mode	$\mathcal{S}$	$\overline{\mathcal{S}}$	$\mathcal{A}_{\rm CP}$	90% CL interval
$K\pi^0$	16.8 ± 7.5	28.9 ± 7.5	$-0.27 \pm 0.23 \pm 0.05$	$[-0.70, 0.16]$
$K^0_S\pi$	14.5 ± 4.4	10.2 ± 4.0	$0.17 \pm 0.24 \pm 0.05$	$[-0.27, 0.61]$
$K\pi$	$38.6^{+9.0}_{-8.1}$	$41.6^{+8.9}_{-8.0}$	$-0.04 \pm 0.16 \pm 0.05$	$[-0.35, 0.27]$
$\eta' K$	51.7 ± 9.2	48.7 ± 8.9	$0.03 \pm 0.12 \pm 0.05$	$[-0.22, 0.28]$
$\omega\pi$	$9.4^{+4.9}_{-4.0}$	$19.1^{+6.8}_{-5.9}$	$-0.34 \pm 0.25 \pm 0.05$	$[-0.80, 0.12]$

Table 3: $\mathcal{A}_{\rm CP}$ measurements in five charmless B decay modes. CLEO 1999 Preliminary.

The search for CP violating asymmetries will intensify with the new datasets expected in the coming years. The precision of such searches will be statistics limited and should improve with integrated luminosity as $1/\sqrt{\mathcal{L}}$. If modes with large asymmetries and reasonable branching ratios exist they could be found within a few years.

References

[1] For a recent review see "CP Violation and Rare Decays of K and B Mesons", A.J. Buras, Lectures given at the 14th Lake Louise Winter Institute, February 1999. hep-ph/9905437

[2] "A Measurement of $\sin 2\beta$ from $B \to J/\psi K_s$ with the CDF Detector"; http://www-cdf.fnal.gov/physics/new/bottom/cdf4855/cdf4855.html

[3] "Measurement of the CP Violation Parameter $\sin 2\beta$ in $B^0 \to \overline{B^0} \to J/\psi K^0_s$ Decays, CDF Collaboration, Phys. Rev. Lett. **81**, (1998), 5513

[4] "Investigation of CP Violation in $B^0 \to J\psi K_s$ Decays at LEP", OPAL Collaboration, Euro. Phys. J. **C5** (1998) 379.

[5] "Rare B Physics at CLEO" A. Lyon, Proceedings of the 1999 Rencontres de Moriond (Electroweak). Also, "$b \to s\gamma$ Branching Fraction and CP Asymmetry", CLEO Collaboration, CLEO CONF 99-10.

[6] "CP violating Asymmetries in Charmless Non-leptonic Decays $B \to PP$, PV, VV in the Factorization Approach", A. Ali, G. Kramer, and C.D. Lü; Phys. Rev. **D**59 (1999) 014005 [hep-ph/9805403]

[7] "Combining CP Asymmetries in $B \to K\pi$ Decays", M. Gronau and J.L. Rosner, Phys. Rev. **D**59 (1999) 113002; [hep-ph/9809384]. It is worth pointing out also that even within the context of factorization where strong phases come strictly from short distance physics, asymmetries as large as 0.5 or greater are predicted in some modes (see previous reference).

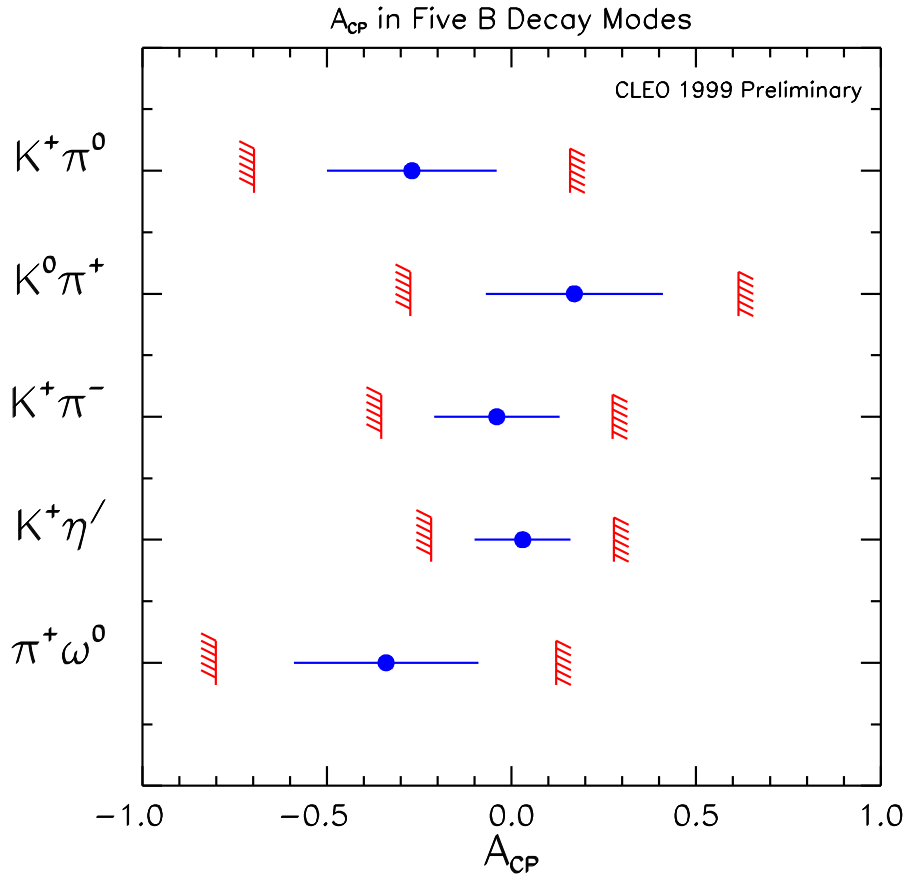

Figure 6: Results for $\mathcal{A}_{\rm CP}$ in five charmless B decay modes. The data points show the central value with 1σ error bars; hatching indicates the range of the 90% CL interval.

[8] See reference 5, above; and "The Possibility of Large Direct CP Violation in $B \to K\pi$-like Modes Due to Long Distance Rescattering Effects and Implications for the Angle γ" D. Atwood and A. Soni, Phys. Rev. **D**58 (1998) 036005; [hep-ph/9712287]; as well as "Model Independent Analysis of $B \to \pi K$ Decays and Bounds on the Weak Phase γ, M. Neubert, JHEP 9902 (1999) 014; [hep-ph/9812396]

[9] CLEO Collaboration, papers submitted to this conference.

[10] Y. Kubota *et al.* (CLEO Collaboration), Nucl. Instrum. Methods Phys. Res., Sec. A**320**, 66 (1992); T. Hill, 6th International Workshop on Vertex Detectors, VERTEX 97, Rio de Janeiro, Brazil.

[11] S. L. Wu, Phys. Rep. C**107**, 59 (1984).

[12] R. Brun *et al.*, GEANT 3.15, CERN DD/EE/84-1.

[13] D. M. Asner *et al.* (CLEO Collaboration), Phys. Rev. D **53**, 1039 (1996).

[14] G. Fox and S. Wolfram, Phys. Rev. Lett. **41**, 1581 (1978).

[15] CLEO Collaboration, R. Godang *et al.*, Phys. Rev. Lett. **80**, 3456 (1998); CLEO Collaboration, paper contributed to this conference.

[16] CLEO Collaboration, B. H. Beherens *et al.*, Phys. Rev. Lett. **80**, 3710 (1998); CLEO Collaboration, paper contributed to this conference.

[17] CLEO Collaboration, T. Bergfeld *et al.*, Phys. Rev. Lett. **81**, 272 (1998); CLEO Collaboration, paper contributed to this conference.